Scientia Iranica D (2014) 21(6), 2153–2164

SCIENTIA IRANICA

Sharif University of Technology
Scientia Iranica
Transactions D: Computer Science & Engineering and Electrical Engineering
www.scientiairanica.com

Bi-level fuzzy force shaping controller of a flexible wiper system

A. Zolfagharian[a,*], A. Noshadi[b] and M.Z. Md. Zain[a]

a. *Department of System Dynamics & Control, University Technology Malaysia, Johor, Malaysia.*
b. *School of Engineering and Science, Faculty of Health, Engineering and Science, Victoria University, Melbourne, Victoria, Australia.*

Received 18 July 2012; received in revised form 25 August 2013; accepted 15 April 2014

KEYWORDS
Automotive wiper;
System identification;
Intelligence control;
Multi-objective optimisation.

Abstract. In flexible manipulators, the residual vibration and unwanted transient deflection are critical issues that are highly correlated with the velocity operation of the system; as the velocity increases the control of such systems become more delicate and difficult. The wiper blades of automobiles are among those types of flexible system that are required to be operated at quite high velocity to be efficient under high load conditions. This causes some annoying noise and deteriorated vision for travellers. The modelling and control of the vibration and low frequency noise of an automobile wiper blade is the focus of this study. The flexible vibration and noise model of a wiper system is estimated using an artificial intelligence system identification approach. A controller approach is also developed to suppress the low frequency noise of a wiper end-point, while maintaining the desired position accuracy of the hub angle, simultaneously.

© 2014 Sharif University of Technology. All rights reserved.

1. Introduction

Flexible structures are broadly utilized in diverse industrial research and design due to their advantages, like free friction loss in joints, low weight, less energy consumption and low cost. Nonetheless, control of flexible manipulators has always been a crucial issue to convince designers to apply them rather than the traditional rigid counterparts in design. However, in some products, like automobile wiper systems, flexibility is an inherent characteristic that cannot be alternated. A wiper system is an indispensible part of an automobile with a flexible nature. The flexibility features of a wiper blade structure have made it a critical apparatus despite its simple operational mechanism. A desirable wiper system is characterized by homogeneous disposal of water, without noise generation, and by limiting, as much as possible, the phenomenon of wear (loss of wiping or noise presence). An experimental method verified with a finite element analysis is carried out for past processing system identification and control of a wiper system [1]. Low frequency noise, known as chatter noise, is identified in a wiper system during operation, which is subject to suppression while not violating other oscillatory attributions of the wiper system in the time domain. This noise is an annoyance for automobile occupants, especially in heavy rain and snow.

The vibration control of chaotic motion in a two blade wiper system was investigated by Wang and Chau [2]. Friction effects between the windscreen and wiper blades and their variation in accordance to the temperature, as well as velocity, of the wiper motor were investigated [3,4]. Inverse dynamics control in co-operation with input shaping was developed to achieve minimum vibration within the bounded speed of the

*. *Corresponding author. Tel.: +98 911 3145289; Fax: +981125232587*
E-mail addresses: ali.zolfagharyan@gmail.com (A. Zolfagharian); amin.noshadi@live.vu.edu.au (A. Noshadi); zarhamdy@fkm.utm.my (M.Z. Md. Zain)

drive [5]. Singla proposed a hybrid control method for a flexible inverted pendulum on a moving car that deals with the vibration of a system with minimum actuator effort [6]. Yanyan et al. [7] proposed a control approach by sensing the extent of rain on a windscreen using an infrared rain sensor that commands motor velocity proportionally. Several methods, like dither signal, extended time-delay feedback control and optimized command shaper control methods, were applied for controlling the chaotic motion of wiper blades [2-8].

The flexible dynamic of a wiper system requires a reliable system identification method to model its transfer function for helping the designer to develop a more accurate controller. Modeling of a wiper system, as a flexible manipulator with several modes, needs a trustworthy system identification method featuring the capability of fast varying dynamics and non-minimum phase systems modeling [9,10]. A nonlinear auto regressive exogenous (NARX) [11] in cascade with the Elman Neural Network (ENN) [12] is utilized for the purpose of the system identification of a nonlinear wiper system.

The Input Shaping (IS) method is a sensor free and effective feed-forward controller chosen for noise reduction and for improving other dynamic characteristics of a flexible wiper blade [13]. The input shaping approach highly depends on system natural frequencies and damping ratios. Employing this method signifies the necessity of precise system identification. Comparative studies of the responses of flexible manipulators by various feed-forward controller techniques were undertaken by Azad et al. [14]. The results proved the superiority of the input shaping technique, in terms of vibration reduction at the first three modes, settling time and overshot, over the Gaussian shaped and low-pass filtered input torque. Also, though the Gaussian method had a better performance in terms of attenuation of Power Spectral Density (PSD) compared to low-filtered input torque, it performed worse based on time response criteria.

In order to handle the performance of a control system within uncertain circumstances, traditional controllers, such as Proportional, Integrative and Derivative (PID) controllers, are not the best choice due to constraints imposed on gains regulations. A Fuzzy Logic Controller (FLC) has the advantage of being able to control a system by means of expert knowledge, and regardless of the actual dynamic of the plant [15]. Some applications of FLC in flexible link control system identification and parallel manipulator control problems can be found in literature [16,17]. Also, some efforts were made to link FLC with evolutionary and swarm approaches [16-18].

In multi-objective control problems, it is necessary to estimate a number of parameters or gains for the control scheme that, in turn, introduces more complexity to the scheme. To tackle this, MOGA is utilized in a control loop in order to attain a trade off solution. A Multi-Objective Genetic Algorithm (MOGA) using a fitness sharing technique is adopted in this study, due to its versatile character when dealing with various conflicting objectives and their constraints. MOGA, based on fitness sharing, has been successfully applied to other control engineering problems regarding flexible manipulators [19,20].

The lack of exotic techniques that target the vibration and noise reduction of wiper blades in both time and frequency domains, simultaneously, encouraged this research. A reliable nonlinear system identification, namely (NARXENN), was adopted in first stage of this survey to model the flexible dynamics of a wiper blade with acquired experimental data. A Zero-Vibration-Derivative-Derivative (ZVDD) IS controller was designed based on the dynamics properties of a wiper system, extracted from system identification and applied to the path of the reference input. Then, closed loop control integrating, FLC and AFC, were developed to add a robust trait to the controller for possible uncertainty that may occur during the operation of the wiper. In order to deal with the complexity of controlling the multi conflict objectives in both time and frequency domains, MOGA is utilized to regulate the corresponding parameters of the proposed controller. Details of the proposed controller are illustrated in Figure 1.

This paper presents data acquisition and the experimental set up in Section 2. Also, a mathematical and conceptual explanation of system identification and control strategies is briefly described. The effectiveness and results of applying the proposed controller are discussed in Section 3. The paper concludes in Section 4.

2. Methodology

2.1. Data acquisition

First, the data acquisition stage is carried out online for recording the wiper system signals. Then, the data analyses run off-line and handle the recorded data to develop an efficient controller, standing by experimental tests.

A uni-blade type wiper, which is typically found

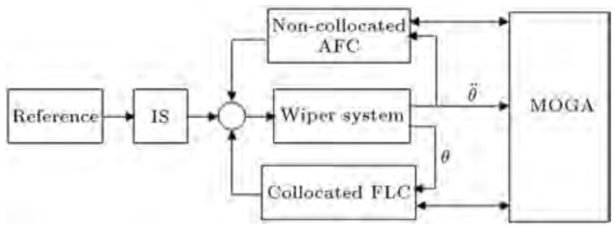

Figure 1. Bi-level active shaper fuzzy force controller using MOGA.

in the Proton Iswara, driven by its corresponding DC Wiper Motor in hub, measuring devices, interface card and digital processor, are used for the experiment. The wiper blade can be considered a pinned-free flexible arm that moves freely in the horizontal plane of windscreen, while the effect of axial force is negligible. A pipe hose with running water is facilitated at the top of the windscreen that simulates rainy or wet conditions for operating the wiper at a speed of Bang-Bang input. The measurement sensors includ a Kistler Type 8794A500 tri-axial accelerometer mounted at the endpoint of the wiper blade, using beeswax for measurement of endpoint acceleration, as well as a shaft encoder placed at the hub of the wiper for measurement of hub angle. Recording the input signals is carried out at digital sampling rate of 1 kHz. In the experiment, a 16 input channels PAK MK II Muller BBM signal analyzer was used.

Simulation of the flexible manipulator is conducted with two analogue outputs, namely, hub angle and end-point acceleration. Low-Pass (LP) filters, each with a cut-off frequency of 80 Hz, are used to band limit the system response to the first resonance mode for each output. Furthermore, to decouple the flexible motion control loop from the rigid body dynamics, a high-pass filter for each output with a cut-off frequency of 5 Hz is used. The system damping ratio is negligible and payload is measured as 7.4 N/m. A motor drive amplifier (current amplifier) delivers a current proportional to the input voltage for actuating a bi-directional motor. A linear drive amplifier LA5600 can be employed as the motor driver, too. The shaft encoder, placed on the hub of the wiper, sends the analogue information of the hub angle of the wiper to the process unit of the controller after being converted to digital values. An interface circuit PCL 812PG is needed to interface the wiper system with a host PC, which carries out data acquisition and control between the processor, the actuator and sensors with 25 μs for A/D conversion and a settling time of 20 μs for D/A conversion. A schematic diagram of the proposed controller interface used in this work is shown in Figure 2.

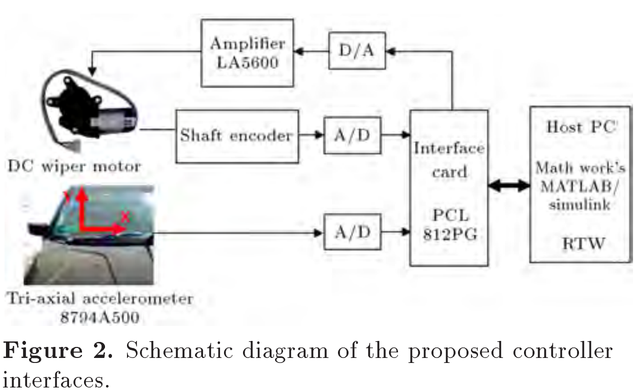

Figure 2. Schematic diagram of the proposed controller interfaces.

2.2. Nonlinear Auto Regressive Exogenous Elman Neural Network (NARXENN)

The NARX model structure is defined by:

$$y(k) = F\left(y(k-1), ..., y(k-n_y), u(k-1), ..., u(k-n_u)\right) + \varepsilon(k), \tag{1}$$

where the effect of noise is assumed additive at the output of the model. $F(.)$ is a nonlinear function, y_k, u_k, and ε_k are output, input, and noise, respectively, where n_y and n_u are maximum lags on observations and exogenous inputs [11]. In order to identify the NARX model, the corresponding $F(.)$ function should be approximated first. In this study, the nonlinear function, $F(.)$, is estimated by ENN.

In the structure of an ENN, there is an additional undertake layer, called the context layer besides the three conventional layers, namely, input, hidden and output layers, that identify the dynamic characteristics [12]. Suppose an ENN, such as shown in Figure 3, in which the vectors of input, middle and output layer nodes are labeled with u, x and y, respectively. Also, W_1, W_2 and W_3 represent the respective connection weights of input, middle and output layers. The nodes of the input layer play the role of signal transmission, while the nonlinear functions of $M(.)$ and $O(.)$ are introduced as transfer functions of middle and output layers. In this study, the tansigmoid function is used. Furthermore, the previous moment output values of the hidden layer were stored in the memory and returned to the input, so, it can be considered a step delay operator. The mathematical modeling of the Elman Neural Network can be expressed as the following equations:

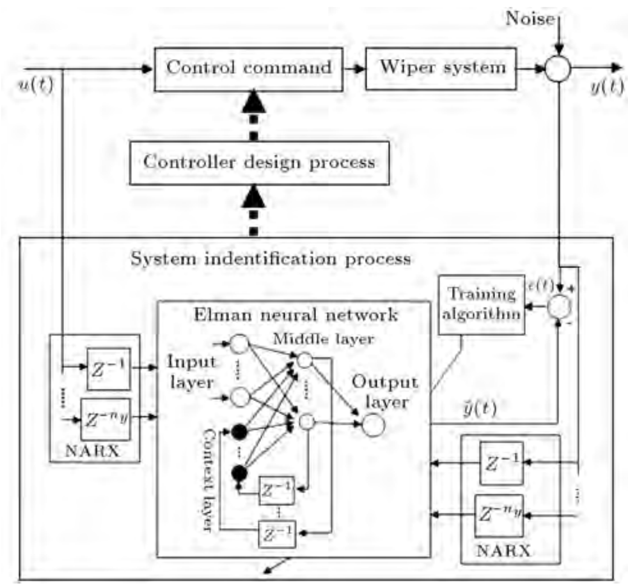

Figure 3. NARXENN system identification of wiper system.

$$X(k) = M\left(W_2.u(k) + W_1.u(k-1)\right), \tag{2}$$

$$Y(k) = O\left(W_3.x(k)\right). \tag{3}$$

A Back Propagation (BP) algorithm, as broadly used and discussed in literature, was adopted for the training process of the neural network. BP uses the error sum of squares function between the output of the network and target values [21]:

$$E(W) = \sum_{n=1}^{k} [y_n(W) - T_n(W)]^2, \qquad n = 1, 2, 3, ..., k, \tag{4}$$

where $T_n(W)$ is the target vector of the output.

A schematic model of the proposed system identification, named a Nonlinear Auto Regressive Elman Neural Network (NARXENN), is illustrated in Figure 3.

2.3. Non-collocated control

The AFC technique is verified to be quite effective in robust accuracy positioning tasks, despite possessing a trouble-free mathematical algorithm [22].

Investigations into applying AFC as a non-collocated control technique showed that by using this method, a system subjected to environmental uncertainties and disturbances remains stable and robust. The successful operation of the AFC method as a disturbance rejecter scheme, compared to traditional control methods, such as the PID controller, is proven in the literature [17,21].

Other advantages of the application of AFC as a disturbance rejector in this study are its low computational burden and less input information required in a real time system. As shown in Figure 4, AFC requires only the acceleration information of the wiper tip.

In rotational bodies, Newton's second law expresses that the sum of all torques applied to the system is equal to the multiplication of the mass moment of (I) to the angular acceleration (α) of the system, i.e. from considering the well-known and functional second Newton law of motion for rotational bodies, as:

$$\sum \tau = I\alpha, \tag{5}$$

where τ is the applied torque of the wiper motor, and I and α are the mass moment of inertia and the angular acceleration of the wiper blade, respectively.

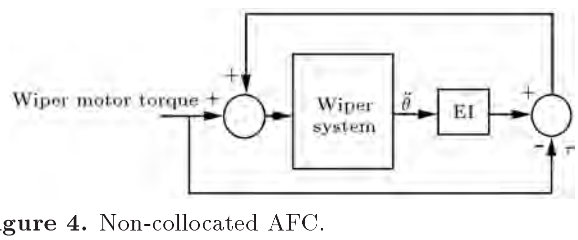

Figure 4. Non-collocated AFC.

An external disturbance, τ_d, is included in Eq. (1):

$$\tau + \tau_d = I(\theta)\alpha. \tag{6}$$

The main point of AFC is when disturbances have to be estimated somehow as:

$$\tau_d^* = \tau - \mathrm{EI}\alpha, \tag{7}$$

where EI is the estimated inertia matrix that can be obtained by crude approximation or other intelligent methods, such as iterative learning, fuzzy logic and so on. MOGA has been used in this paper to estimate the most appropriate value for EI to achieve a desirable trade off among all objectives, even in the presence of external disturbance. τ is the measured applied control torque that can be estimated by a current sensor or directly by a force or torque sensor and the measured angular acceleration, $\ddot{\theta}$ can be obtained by an accelerometer. From Eq. (7), it is clear that if the total applied torque to the system and angular acceleration of each actuated joint are accurately obtained using measuring instruments, and the estimated inertial parameters needed in the AFC loop for disturbance rejection are appropriately approximated, without having to acquire knowledge about the actual magnitude of the disturbance, the total torque disturbances can be rejected using the AFC loop. A schematic diagram of the developed AFC method, as part of the proposed controller, is depicted in Figure 4.

2.4. Collocated controller

A fuzzy controller with two inputs, named, the track error and rate of track error of the wiper hub displacement, and one output, which is in the path of a scale factor, is adopted in the collocated control part (Figure 5). The inputs and output of the fuzzy controller are normalized within the range of $[-1, 1]$, while the appropriate location of membership function inputs, as well as scale factor parameters, have been tuned by MOGA for normalization purposes, based on the following conditions:

$$\mathrm{TE} = \max\left(-1, \min(1, S_{\mathrm{TE}})\right), \tag{8}$$

$$\delta\mathrm{TE} = \max\left(-1, \min(1, S_{\delta\mathrm{TE}})\right), \tag{9}$$

where TE and δTE represent the track error and rate of track error for hub displacement of the wiper

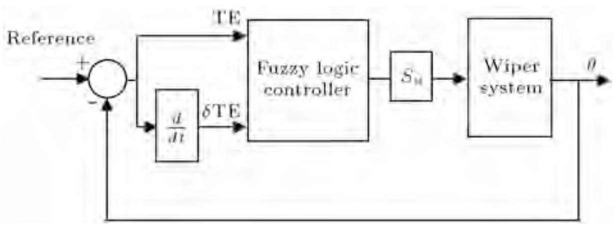

Figure 5. Collocated FLC.

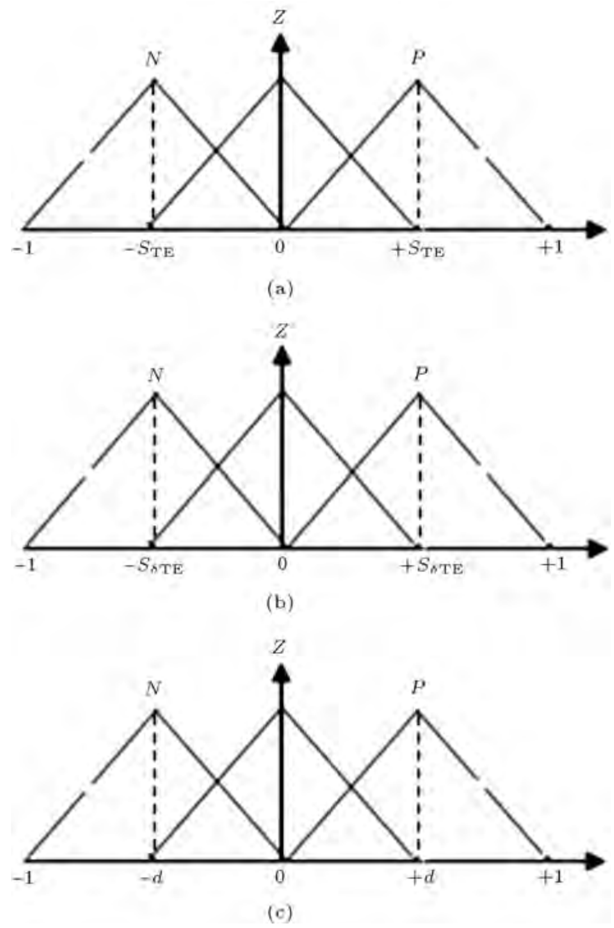

Figure 6. Membership functions illustration of FLC: (a) Track error input; (b) rate of track error input; and (c) controller output.

respectively. S_{TE} and $S_{\delta\mathrm{TE}}$ are the best position of the membership functions of TE and δTE, which are aimed to be adjusted by MOGA. Similarly, the FLC output is denormalized using $U = S_u.\hat{u}$. Membership functions of the inputs and output of the fuzzy logic controller are shown in Figure 6.

The different values of S_{TE} for track error, and $S_{\delta\mathrm{TE}}$ for rate of track error of the controller lead to various shapes of triangles. Since the FL output is manipulated by the S_u factor, which is fine tuned by MOGA, the positions of the output membership function ($\pm d$) are supposed to be constant at $d = \pm 0.5$.

For the two inputs, as well as the output, of the FLC, five triangle membership functions were chosen for each, and a complete rule matrix of size 5×5 is defined in Table 1.

The nth command of the rule base for the FLC with track error and rate of track error, as fuzzy inputs, and $\hat{u}$ as fuzzy output is given by:

C_n: If TE is NB and δTE is ZE then the $\hat{u}$ is PB.

A two level fuzzy tuning method whose normalized

Table 1. FLC rule base with track error and rate of track error.

Track Error (TE)	**Rate of Track Error (δTE)**		
	N	Z	P
N	P	P	Z
Z	P	Z	N
P	Z	N	N

output parameter (S_u) as well as nonlinear tuning parameters (S_{TE}) and ($S_{\delta\mathrm{TE}}$) are adjusted by means of MOGA, is developed. The superiority of the proposed controller in similar work is tuning of the nonlinear parameters of the FL input membership, which increase the robustness and performance of the controller without exceeding the maximum permitted value of the S_u scale factor.

2.5. Open-loop input shaping control

An input shaping mathematic derivation for a two-impulse sequence can be obtained as follows. The transfer function of a second order system, whose nth natural frequency and damping ratio are ω_n and ξ, respectively, can be stated as follows:

$$T(s) = \frac{\omega_n^2}{s^2 + 2\xi\omega_n s + \omega_n^2}. \tag{10}$$

The residual vibration resulted from a series of impulses utilized in the system can be derived from the second order system transfer fuction as [13]:

$$V(\omega,\xi) = e^{-\xi\omega_n}\sqrt{\left(\sum_{i=1}^{N} P_i(\omega,\xi)\right)^2 \left(\sum_{i=1}^{N} Q_i(\omega,\xi)\right)^2}, \tag{11}$$

$$P_i = A_i e^{-\xi\omega t_i}\cos\left(\omega_n\sqrt{1-\xi^2}t_i\right),$$

$$Q_i = A_i e^{-\xi\omega t_i}\sin\left(\omega_n\sqrt{1-\xi^2}t_i\right), \tag{12}$$

where A_i is amplitude, t_i represents the time of the impulses and n is the number of impulses in the impulse sequence.

As the number of impulse shapers increases, the controller becomes more robust due to the increase in rise time. So, the number of impulse shapers is a compromise, which is determined based on design specifications. A ZVDD input shaper that is comprised of a four-impulse shaper is employed in this study. The time and location of a four impulse ZVDD is listed in Table 2.

In this study, first the natural, frequency of a wiper system is inferred from the results of data acquisition and system identification as, approximately, 11 Hz. Also, the damping ratio of the wiper system is estimated, using finite element analysis, as 0.16 [23].

Table 2. Magnitude and time location of four-impulse IS (ZVDD).

i	A_i	t_i
1	$\frac{1}{(G+1)^3}$	0
2	$\frac{3G}{(G+1)^3}$	$\frac{Td}{2}$
3	$\frac{3G^2}{(G+1)^3}$	Td
4	$\frac{G^3}{(G+1)^3}$	$\frac{3Td}{2}$

2.6. MOGA

Fitness sharing based MOGA is utilized to give confidence in the search towards the true Pareto optimal set while maintaining diversity in the population [24]. The basic idea of fitness sharing is that all individuals within the same region (called a niche) share their fitness. In the fitness sharing method, first, a niche count is obtained from the Euclidean distance between every solution pair and then the fitness of each solution is assigned from the best individual to the worst, according to some function in the form of a fitness function, such as linear or exponential, or, possibly, other types. The greater fitness is understood here to be the number of individuals decreased in the same rank. The stochastic universal sampling method is used to select the best individuals [25]. However, mating restrictions are employed in order to protect from lethal [26]. In a multi-objective Pareto based optimization problem, it shall be assumed that the true Pareto front is unknown. Therefore, the only means of evaluation available is to compare the MOGA solutions against each other. A hypervolume indicator is adopted in this study for performance assessment of MOGA [27].

3. Results and discussions

3.1. Multi-objectives indexes

Three objectives of a wiper system's dynamic characteristics are defined and considered in this study. The Integral of Absolute End-point Acceleration (IAEA), maximum overshot of hub displacement and rise time of hub displacement response are objectives that are aimed to be minimized and defined as:

- Integral absolute value of end-point acceleration (IAEA):

$$\mathrm{IAEA} = \int_0^T |y_{\mathrm{EA}}(t)| dt, \tag{13}$$

  where $|y_{\mathrm{EA}}(t)|$ denotes the end-point acceleration of the wiper blade. IAEA integrates the area of acceleration response of a wiper blade, with respect to time. IAEA is an index of the noise level of a wiper blade.
- Rise time: The time required for the system hub displacement response to rise from 5% to 95% of the final steady state value of the desired response.
- Maximum overshoot: The maximum peak value of the hub displacement response curve measured from the desired response of the system.

In the engineering field, designers frequently come across trade-off problems. In the design of the proposed bi-level fuzzy force shaping controller, such a trade-off emerges in the relationship between rise time and vibration amplitude. Typically, in a flexible manipulator and structure dynamics control, often, the low levels of residual vibration cannot be obtained with a command that produces the fastest rise time [28,29]. In most cases, to achieve low levels of vibration and highest robustness, the rise time must be increased, which is not desirable. IAEA and maximum overshoot are objectives in accord while the rise time index of the wiper lip is in obvious conflict with the two aforementioned objectives.

3.2. System identification

For the modeling process, input-output data were collected for a wiper system. Then, performing one value at the moment, the best maximum lag of the data in the NARX model was found to be $n_x = n_y = 7$. Subsequently, ENN, with two hidden layers, each with 10 tansigmoid neurons and two linear output layers, was trained. The process is adjusted until the prediction output satisfies a model validation test and the model Mean Squared Error (MSE) level reaches 0.000048. The fitting accuracy of the predicted system for One Step Ahead (OSA) prediction of the corresponding end-point acceleration and hub-angle responses of the actual system, compared to NARXENN, are shown in Figure 7.

The illustrated results of actual and predicted PSD and Yule Walker power/frequency of end-point acceleration in the frequency domain in Figure 8 prove that there is an acceptable comparison between system identification results and actual results in the frequency domain, as well.

3.3. Input shaping controller for single objective

First, ISC is designed, based on the extracted natural frequency, and the damping ratio of the wiper model is applied to the system. Figures 9 and 10 show the IS controller is capable of reducing vibration and noise at the end-point of the manipulator in an open-loop control, without the intervention of any external disturbance.

Nonetheless, further study revealed the deficiency of the IS controller in vibration and noise elimination of a wiper blade in the presence of external disturbance and uncertainty (Figure 14). Hence, the essence of an effective controller for reduction of the

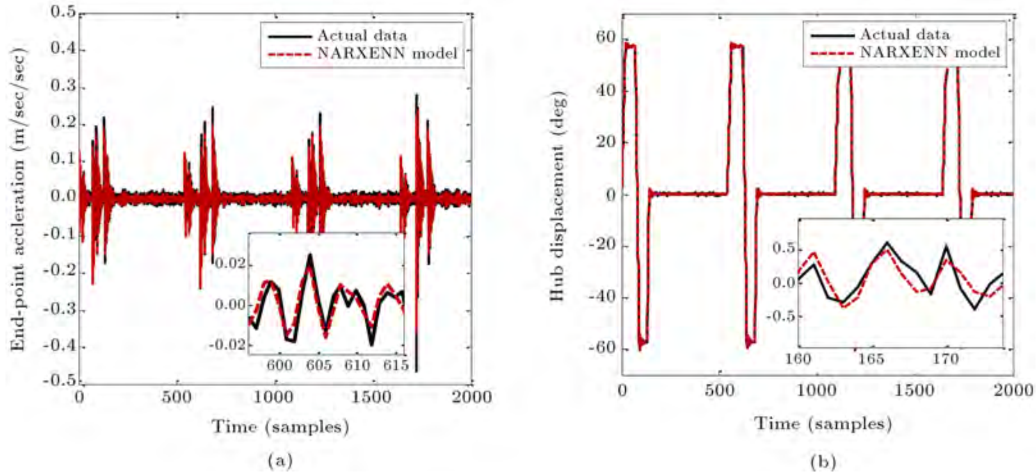

Figure 7. Time domain modeling of wiper lip response: (a) End-point acceleration of wiper lip; and (b) hub displacement.

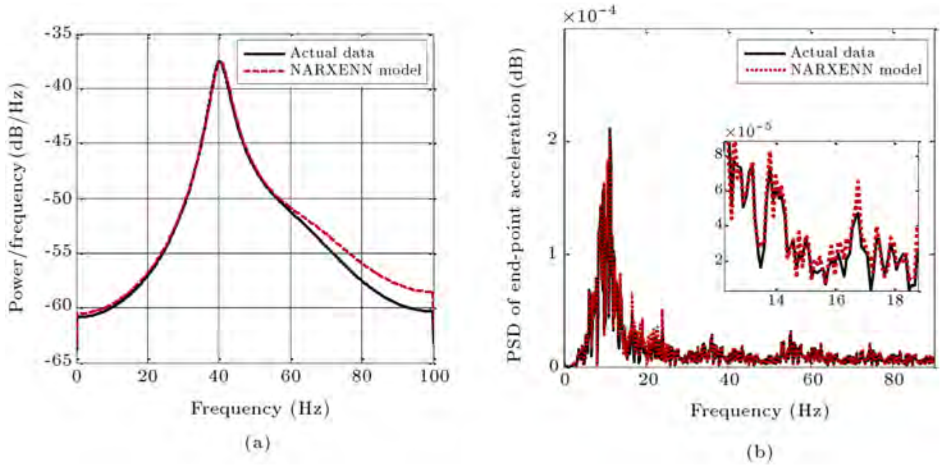

Figure 8. Frequency domain modeling of wiper lip response: (a) PSD of end-point acceleration; and (b) Yule-Walker spectral density of end-point acceleration.

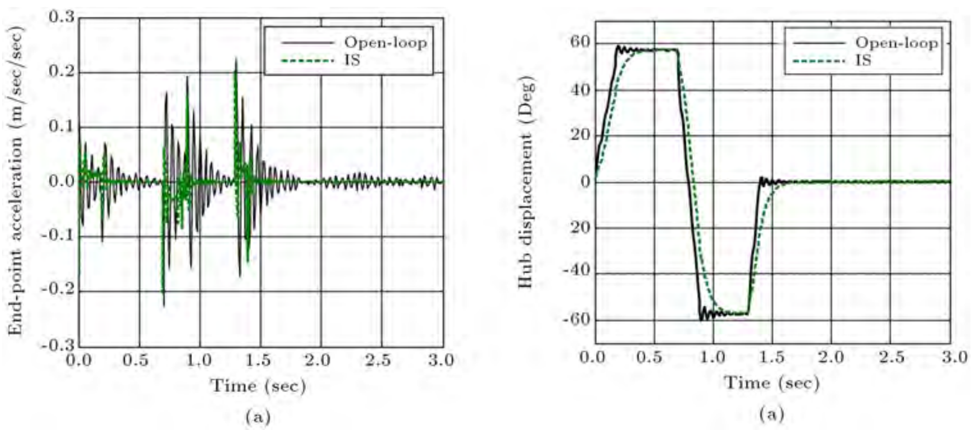

Figure 9. Time domain response of wiper lip without disturbance: (a) End-point acceleration of wiper lip; and (b) hub displacemen.

chatter noise level of a wiper blade, simultaneously, with accurate trajectory tracking of the wiper hub angle was demanded. In order to achieve such a controller, it is required to add a closed-loop controller for flexural motion control of the system. An extended control structure for control of a flexible wiper blade is devised. In the proposed controller, two different loops of AFC and FLC are accumulated to send the most accurate command to the input torque to reject any unknown external disturbance. The control scheme

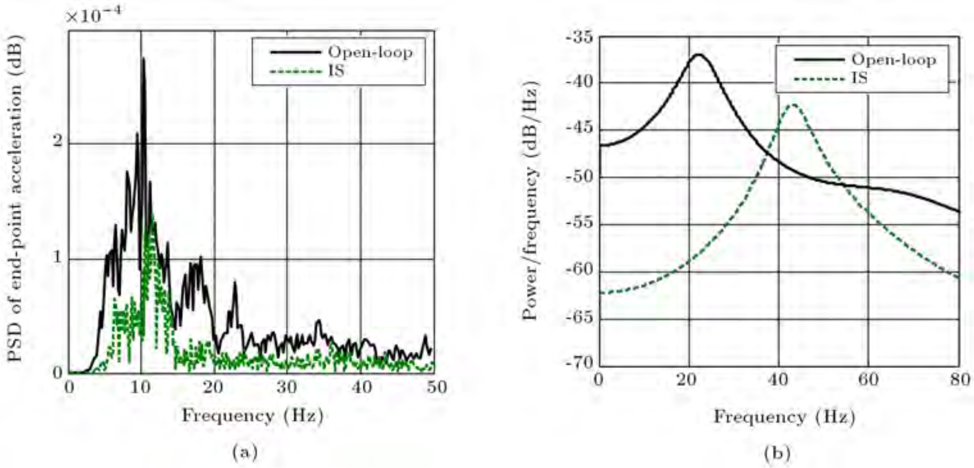

Figure 10. Frequency domain response of wiper lip without disturbance: (a) PSD of end-point acceleration; and (b) Yule-Walker spectral density of end-point acceleration.

has been devised within a simulation environment and is standing by an experimental rig.

In the following investigation, to validate the effectiveness of the proposed controller in the presence of external disturbance, a harmonic disturbance (τ_d) is imposed onto the wiper over time:

$$\tau_d = 2\cos(t). \tag{14}$$

3.4. Bi-level fuzzy force shaping control for multi-objectives

A hypervolume indicator assesses the convergence of an algorithm towards the Pareto front, as well as preserving the distribution of the Pareto front throughout objectives space. In other words, this metric explores the extent of the objective space covered by a set of solutions, which is restricted by setting a suitable reference point. In the case of minimization problems, as in the case of the current paper, the reference point is set in such a way that exceeds the constraint of each objective. Therefore, once this metric is applied to compare the performance of an algorithm in successive iterations (as the number of non-dominated solutions and their distribution throughout the objective space increases), the hypervolume indicator's value represents the greater value.

MOGA is initialized with a random population consisting of 50 individuals and maximum generation of 100 as the termination criterion. The population is represented by binary strings each of 30 bits, called chromosomes. Each chromosome consists of five separate strings. Three terms are specified to FL membership positions, and the remaining two are specified proportional and integrative sale factors of the BFFS controller. Using an educated guess, a reasonable range for these parameters, that ensure the stability of the system, is defined. The crossover rate and mutation rate for this optimization process were set at 90% and 0.01%, respectively. Moreover, the Epanechnikov fitness sharing genetic technique is used to ensure that the best solution of each generation is selected for the next generation, so that the next generation's best will never degenerate and, hence, guarantee convergence of the GA optimization process.

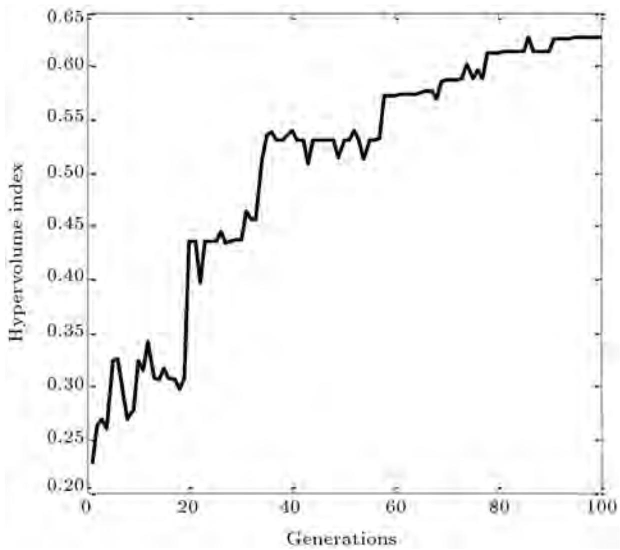

Figure 11. Hypervolume indicator of wiper system objective space using MOGA.

The hypervolume indicator of MOGA for adjusting the controller parameters is shown in Figure 11. It can be clearly seen that the overall number of Pareto front members found in each generation and their diversity throughout the objective space are increased as the number of generations goes on, so that the maximum value of hypervolume is obtained at the last generation.

Explicit conflict interests of maximum overshot and IAEA for Pareto optimal sets of wiper blade objectives are illustrated in Figure 12. This mis-correlation makes the decision tough for designers to

Table 3. Controller parameters and objective values.

Trade no.	Objectives			Controller parameters			
	IAEA m/s^2	Rise time (s)	Max. overshot (%)	S_{TE}	$S_{\delta\text{TE}}$	S_u	EI
1	978	0.11	84	0.517	0.127	0.402	2.940
2	553	0.19	69	0.623	0.594	0.163	3.184
3	178	0.26	27	0.657	0.737	0.127	1.146
4	522	0.20	42	0.118	0.245	0.644	5.637
5	127	0.35	8	0.241	0.172	0.387	2.286

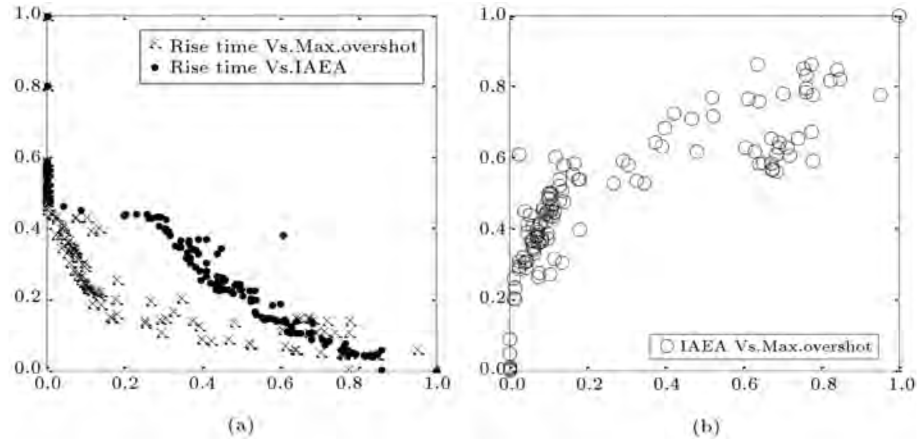

Figure 12. Optimal Pareto sets illustrations of pair objectives: (a) Conflict interests; and (b) mutual interests.

choose the best trade-off. However, the non-dominated Pareto set depicted in Figure 12 proves that IAEA and maximum overshot are highly non-competitive, which is important for the decision maker, as it conceptually reduces the complexity of the problem.

Adjustable parameters of a BFFS controller and their corresponding objective measures are inserted in Table 3. In Table 3, the most significant non-dominated samples of Pareto optimal sets swinging between the robustness performances and rise time improvement of a wiper blade are shown. It can be deduced that the smallest rise time of the system is obtained in Trade 2 with unfavorable IAEA and maximum overshot. Further, the smallest amounts of vibration objectives are achieved in sol. 6 at the expense of the longest rise time. However, in the case of the current design, Trade 3 is deemed to be preferred to the others, which leads to the most reasonable values of IAEA, maximum overshot and rise time of wiper blade. Glimpsing other tradeoffs in Table 3 reveals that though Trade 5 has greater vibration reduction and wiper hub trajectory tracking than Trade 3; this is achieved at the expense of longer system delay or rise time. Also, diverse objectives can be seen in other solutions shown in the table, so that each of them can be obtained by adjusting the location of membership functions, as well as corresponding scale factors of AFC.

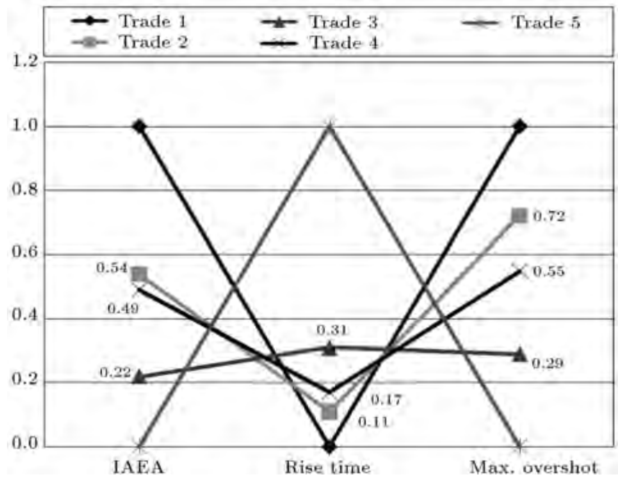

Figure 13. Trades off samples among three objectives' Pareto set.

An instances trade off of Pareto front sets for IAEA, rise time and maximum overshot of a wiper blade is shown in Figure 13. The x axis shows the design objectives and the y axis signifies normalized values of each objective. The conflict interests of objectives are deduced from crossing lines between adjacent objectives, while parallel lines are evidence of mutual interest between the objectives.

According to the major task of the proposed controller in obtaining the greatest vibration and noise

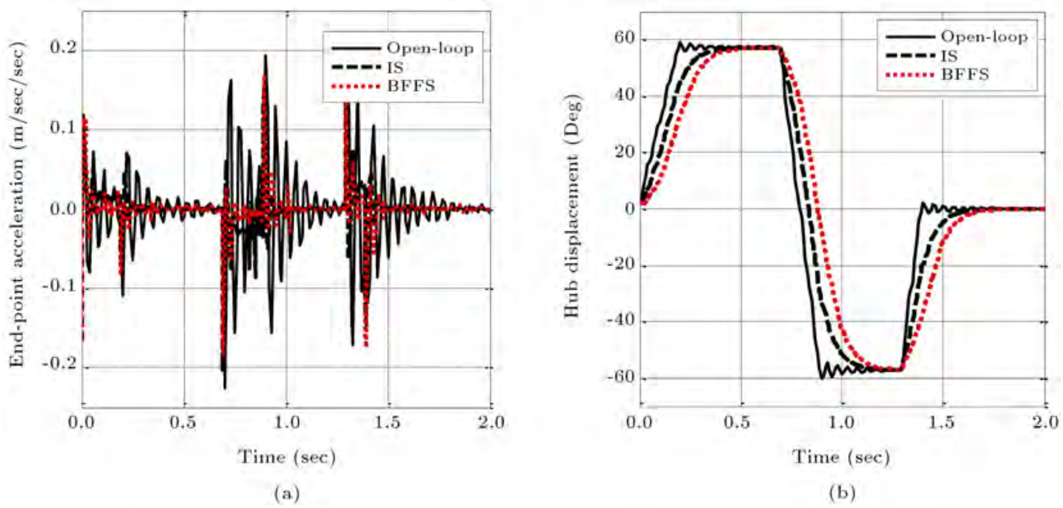

Figure 14. Time domain response of wiper lip in presence of disturbance: (a) End-point acceleration of wiper lip; and (b) hub displacemen.

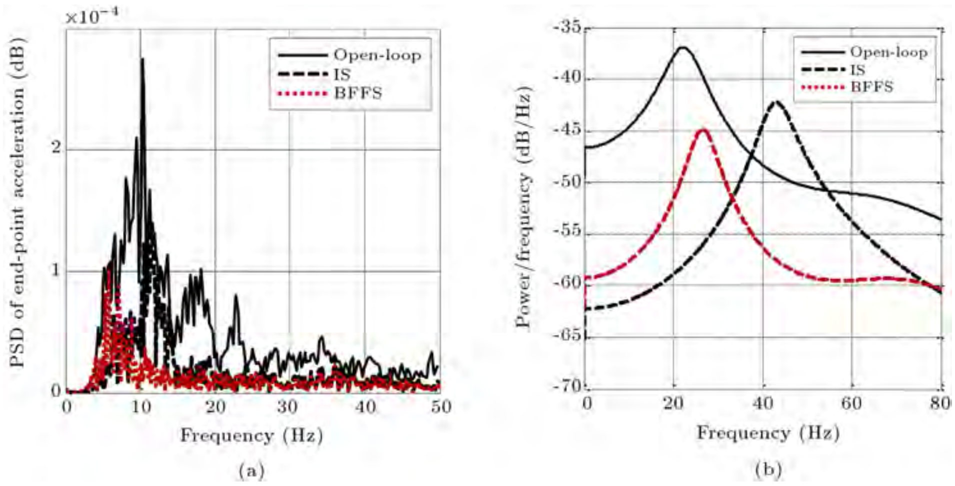

Figure 15. Frequency domain response of wiper lip in presence of disturbance: (a) PSD of end-point acceleration; and (b) Yule-Walker spectral density of end-point acceleration.

reduction of wiper blades in the frequency domain, while setting the reasonable rise time of the system concurrently, the designer should vote on behalf of Trade 3, with the estimated values of IAEA, maximum overshot and rise time of wiper blade 178, 27 and 0.26 s, respectively.

The robustness of the BFFS controller can be obviously deduced from Figure 14. Figure 14(a) shows the noteworthy dampening of end-point acceleration using the BFFS controller rather than the stand alone IS controller with uncertainty. In Figure 14(b), the high distortion of the open loop wiper lip in tracking the desired trajectory, subject to external disturbance, is evident, while the least fluctuation in minimum rise time has been achieved using the BFFS controller. Moreover, the deficiency of the IS controller in comparison to the proposed controller, when applying external disturbances can readily be seen, in terms of end-point acceleration, rise time and maximum overshot.

The vibration amplitude reduction of the developed controller is shown in Figure 15. PSD and Yule-Walker amplitudes of the wiper end-point that indicate the measure of chatter noise of the wiper system are considerably reduced with the BFFS controller compared to the open-loop and IS controller subjected to external disturbance. Also, performance indexes of various controllers are illustrated in Figure 16.

4. Conclusion

Control of a flexible wiper system is split into two tasks; one is to track the Bang-Bang input of the hub angle as open-loop control, and two, is to reduce chatter noise and the unwanted vibration of wiper blades applying a collocated and non-collocated closed-loop controller. The IS controller is designed based on prior knowledge of a wiper dynamics system from NARXENN system identification. The IS controller was implemented

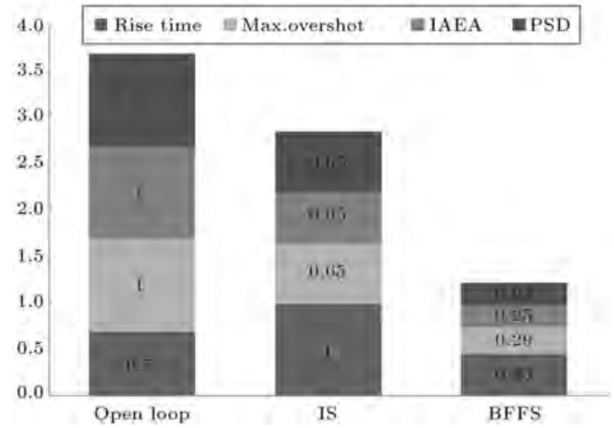

Figure 16. Performance measurements of controllers.

outside the feedback loop and was capable of reducing vibration and noise in a wiper system under free disturbance circumstances. The insensible and deteriorated response of the IS controller to uncertainties persuaded the study to devise a feedback controller. Hence, two level closed loop controllers consisting of collocated FLC and non-collocated AFC were extended. MOGA was applied to achieve the optimum trajectory planning of the wiper hub at a reasonable rise time. It was shown that increasing the robustness to parameter uncertainties does not lengthen the duration of the transient time characteristics.

References

1. Awang, I.M., AbuBakar, A.R., Ghani, B.A., Rahman, R.A. and Zain, M.Z.M. "Complex eigenvalue analysis of windscreen wiper chatter noise and its suppression by structural modifications", *Int. J. Vehic. Struc. Syst.*, **1**(1-3), pp. 24-29 (2009).

2. Wang, Z. and Chau, K.T. "Control of chaotic vibration in automotive wiper systems", *Chaos Soliton. Fract.*, **39**, pp. 168-181 (2009).

3. Koenen, A. and Sanon, A. "Tribological and vibroacoustic behavior of a contact between rubber and glass (application to wiper blade)", *Tribol. Int.*, **40**, pp. 1484-1491 (2007).

4. Bodai, G. and Goda, T.J. "Sliding friction of wiper blade: Measurement, FE modeling and mixed friction simulation", *Tribology International*, **70**, pp. 63-74 (2014).

5. Sahinkaya, M.N. "Input shaping for vibration-free positioning of exible systems", *Proc. Instn. Mech. Engrs.*, Vol 215, Part I, *IMechE*, pp. 467-481 (2001).

6. Ashish, S. "Vibration suppression of a cart-flexible pole system using a hybrid controller", *Proceedings of the 1st International and 16th National Conference on Machines and Mechanisms (iNaCoMM2013)*, IIT Roorkee, India, Dec, pp. 18-20 (2013).

7. Yanyan, W., Jiana, W. and Zhifu, Z. "Design of intelligent infrared windscreen wiper based on MCU", *Procedia Engineering*, **15**, pp. 2484-2488 (2011).

8. Zolfagharian, A., Zain, M.Z. Md., Abu Bakar, A.R. and As'arry, A. "Suppressing chatter noise in windscreen wiper operation using a robust hybrid controller", *Int. Rev. Mech. Egr. (I.RE.M.E.)*, **6**(3), pp. 630-635 (2012).

9. Shaheed, M.H. and Tokhi, M.O. "Dynamic modelling of a single-link of a flexible manipulator: Parametric and non-parametric approaches", *J. Robotica*, **20**, pp. 93-109 (2002).

10. Warwick, J.K., Kang, Y.H. and Mitchell, R.J. "Genetic least squares for system identification", *Soft Computing*, **3**, pp. 200-205 (1999).

11. Chen, S. and Billings, S.A. "Representations of nonlinear systems: The NARMAX model", *Int. J. Control*, **49**, pp. 1013-1032 (1989).

12. Elman, J. "Finding structure in time", *J. Cognitive Sci.*, **14**, pp. 179-211 (1990).

13. Singer, N.C. and Seering, W.P. "Reshaping command inputs to reduce system vibration", *Trans. of ASME, J. of Dynamic Systems, Measurement and Control*, **112**(1), pp. 76-82 (1990).

14. Azad, A.K.M., Shaheed, M.H., Mohamed, Z., Tokhi M.O. and Poerwanto, H. "Open-loop control of flexible manipulators using command-generation techniques", In M.O. Tokhi and A.K.M. Azad (Eds.), *Flexible Robot Manipulators Modelling, Simulation and Control*, London, United Kingdom: The Institution of Engineering and Technology, pp. 207-233 (2008).

15. Zadeh, L.A. "Outline of a new approach to the analysis of complex systems and decision processes", *IEEE Trans. Syst. Man Cyb.*, **1**, pp. 28-44 (1973).

16. Alam, M.S. and Tokhi, M.O. "Hybrid fuzzy logic control with genetic optimisation for a single-link flexible manipulator", *Engineering Application of Artifitial Intelligence*, **21**, pp. 858-873 (2008).

17. Noshadi, A., Mailah, M. and Zolfagharian, A. "Intelligent active force control of a 3-RRR parallel manipulator incorporating fuzzy resolved acceleration control", *Appl. Math. Modell.*, **36**(6), pp. 2370-2383 (2011).

18. Chatterjee, A., Pulasinghe, K., Watanabe, K. and Izumi, K. "A particle swarm optimized fuzzy-neural network for voice-controlled robot systems", *IEEE Trans. Ind. Electron.*, **52**(6), pp. 1478-1489 (2005).

19. Silva, V.V.R., Fleming, P.J., Sugimoto, J. and Yokoyama, R. "Multi-objective optimization using variable complexity modelling for control system design", *Appl. Soft Comput.*, **8**, pp. 392-401 (2008).

20. Toha, S.F. and Tokhi, M.O. "A hybrid control scheme for a twin rotor system with multi-objective genetic algorithm", *Proceeding of the 12th International Con-*

ference on Computer Modelling and Simulation, IEEE, pp. 110-115 (2010).

21. Srinivasan, B., Prasad, U.R. and Rao, N.J. "Back-propagation through adjoins for the identification of non-linear dynamic systems using recurrent neural models", *IEEE Trans. Neural Networ.*, **5**(2) pp. 213-228 (1994).

22. Hewit, J.R. and Burdess, J.S. "Fast dynamic decoupled control for robotics using active force control", *Mechanism and Machine Theory*, **16**(5), pp. 535-542 (1981).

23. Zolfagharian, A., Noshadi, A., Khosravani, M.R. and Zain, M.Z. Md. "Unwanted noise and vibration control using finite element analysis and artificial intelligence", *Appl. Math. Modell.*, http://dx.doi.org/10.1016/j.apm.2013.10.039 (2013).

24. Fonseca, C.M. and Fleming, P.J. "An overview of evolutionary algorithms in multi-objective optimization", *Evol. Comput.*, **3**(1), pp. 1-16 (1995).

25. Goldberg, D.E. and Richardson, J. "Genetic algorithms with sharing for multimodal function optimization", In *J. Grefenstette (Ed.), Proceedings of the Second International Conference on Genetic Algorithms*, Hillsdale, NJ: Lawrence Erlbaum Associates, pp. 41-49 (1987).

26. Deb, K., *Multi-Objective Optimization Using Evolutionary Algorithms*, Chichester: Wiley, New York (2001).

27. Zitzler, E. and Thiele, L. "Multi-objective evolutionary algorithms: A comparative case study and the strength Pareto approach", *IEEE Trans. Evol. Comput.*, **3**(4), pp. 257-71 (1999).

28. Tokhi, M.O. and Zain, M.Z.M. "Hybrid learning control schemes with acceleration feedback of a flexible manipulator system", *Proceedings of the Institution of Mechanical Engineers, Part I: Journal of Systems and Control Engineering*, **220**(4), pp. 257-267 (2006).

29. Zain, M.Z. Md., Tokhi, M.O. and Mohamed, Z. "Hybrid learning control schemes with input shaping of a flexible manipulator system", *Mechatronics*, **16**, pp. 209-219 (2006).

Biographies

Ali Zolfagharian was born in Iran, in 1985. He graduated in Mechanical Engineering from the University of Mazandaran, Iran, in 2009, and obtained his MS degree in dynamics, vibration and control from University Technology Malaysia (UTM), in 2011. His area of expertise includes application of various controllers on flexible structures, robotic manipulators, artificial intelligence control and optimization approaches.

Amin Noshadi was born in Iran, in 1983. He obtained his BS degree in Mechanical Engineering from Ferdowsi University, Mashhad, Iran in 2007, and his MS degree from the Department of System Dynamics and Control in the Faculty of Mechanical Engineering at University Technology Malaysia (UTM). He is currently a PhD student in the School of Engineering and Science, Faculty of Health, Engineering and Science, Victoria University, Melbourne, Victoria, Australia. His current research interests include robotics, specifically design and control of parallel manipulators, active force control, iterative learning control, fuzzy systems, genetic algorithm, particle swarm optimization, and neural network based systems.

Mohd Zarhamdy Md. Zain was born in Malaysia. He obtained his BS degree in Mechanical Engineering from University Technology Malaysia (UTM), and his MS and PhD degree, in Control, from Sheffield University, UK Currently, he is senior lecturer in the Department of System Dynamics and Control, at the Faculty of Mechanical Engineering, UTM, Malasia.